Single-molecule imaging of EGFR signalling on the surface of living cells

Yasushi Sako*, Shigeru Minoguchi* and Toshio Yanagida*†‡

**Department of Physiology and Biosignalling, Graduate School of Medicine, Osaka University, 2-2 Yamadaoka, Suita 565-0871, Japan*

†Single Molecule Processes Project, ICORP, JST, 2-4-14 Senba-Higashi, Mino 562-0035, Japan

‡e-mail: yanagida@phys1.med.osaka-u.ac.jp

The early events in signal transduction from the epidermal growth factor (EGF) receptor (EGFR) are dimerization and autophosphorylation of the receptor, induced by binding of EGF. Here we observe these events in living cells by visualizing single molecules of fluorescent-dye-labelled EGF in the plasma membrane of A431 carcinoma cells. Single-molecule tracking reveals that the predominant mechanism of dimerization involves the formation of a cell-surface complex of one EGF molecule and an EGFR dimer, followed by the direct arrest of a second EGF molecule, indicating that the EGFR dimers were probably preformed before the binding of the second EGF molecule. Single-molecule fluorescence-resonance energy transfer shows that EGF–EGFR complexes indeed form dimers at the molecular level. Use of a monoclonal antibody specific to the phosphorylated (activated) EGFR reveals that the EGFR becomes phosphorylated after dimerization.

Single-molecule imaging is an ideal technology by which to study the molecular mechanisms of biological reactions *in vitro*[1–3]. Here we extend this technology to real-time observations of the binding of fluorescent-dye-labelled EGF to its receptor (EGFR), dimerization of EGF–EGFR complexes, and autophosphorylation of EGFR in the plasma membrane. Although dimerization and autophosphorylation are known to be essential for signal transduction of EGFR[4,5], the mechanisms underlying these events have not been fully understood until now.

Results

Visualization of single molecules on the surface of living cells. As a probe for detection of single molecules in living cells, we used a fluorescent dye, Cy3, conjugated to mouse EGF. As mouse EGF has only one reactive amino residue (at the amino terminus), it can be labelled with amino-reactive Cy3 dye with a dye:protein ratio of exactly 1:1.

Under an objective-type total internal reflection (TIR) fluorescence microcope[3], Cy3-labelled EGF (Cy3–EGF) was added to the culture medium of A431 cells (Fig. 1). The background autofluores-

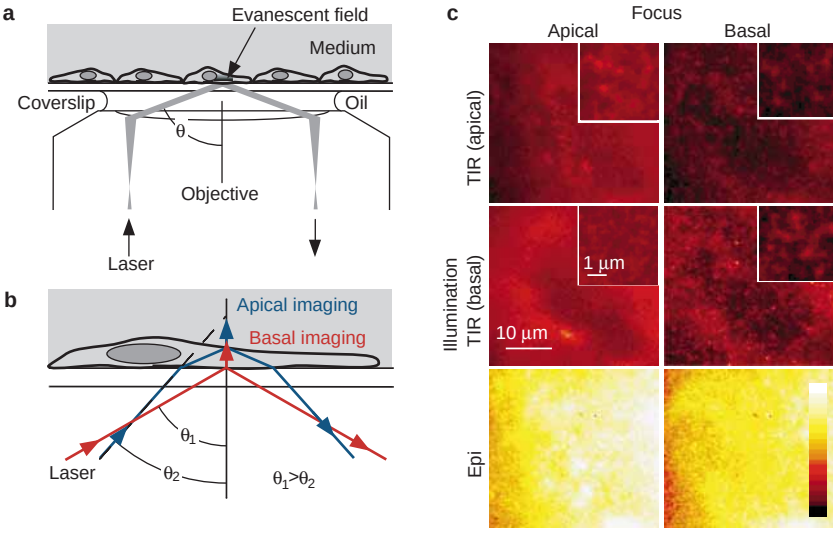

Figure 1 **TIR microscopy for visualization of single molecules on the cell surface. a**, TIR microscopy. An objective-type TIR microscope was used. **b**, For imaging of the basal cell surface, a laser beam was reflected between a coverslip and the culture medium. For imaging of the apical plasma membrane, the incident angle of the laser beam was reduced ($\theta_1 > \theta_2$) and the laser beam was reflected between the cytoplasm and culture medium. **c**, To demonstrate the effect of the illumination mode, images of A431 cells were taken in the same field under different illumination modes in the presence of 100 ng ml^{-1} Cy3–EGF. The cells were 2–3 μm thick, and so, by changing the focus, we could easily distinguish between the apical surface and the basal surface. Under apical TIR mode, fluorescent spots were shown on both apical and basal surfaces. In this case, spots on the basal surface would be excited by epifluoresence illumination. Because of excitation of Cy3–EGF in the basolateral surface and free Cy3–EGF in the evanescent field, background fluorescence was higher on the apical surface than on the basal surface. Even in this condition, individual Cy3–EGF molecules could be visualized on the apical surface (inset). Under basal TIR mode, spots were only observed on the basal surface because of the limited excitation depth of TIR. Under the epifluorescence configuration, background from fluorescent EGF in the culture medium was high and no fluorescent spots on the cell surface were detected.

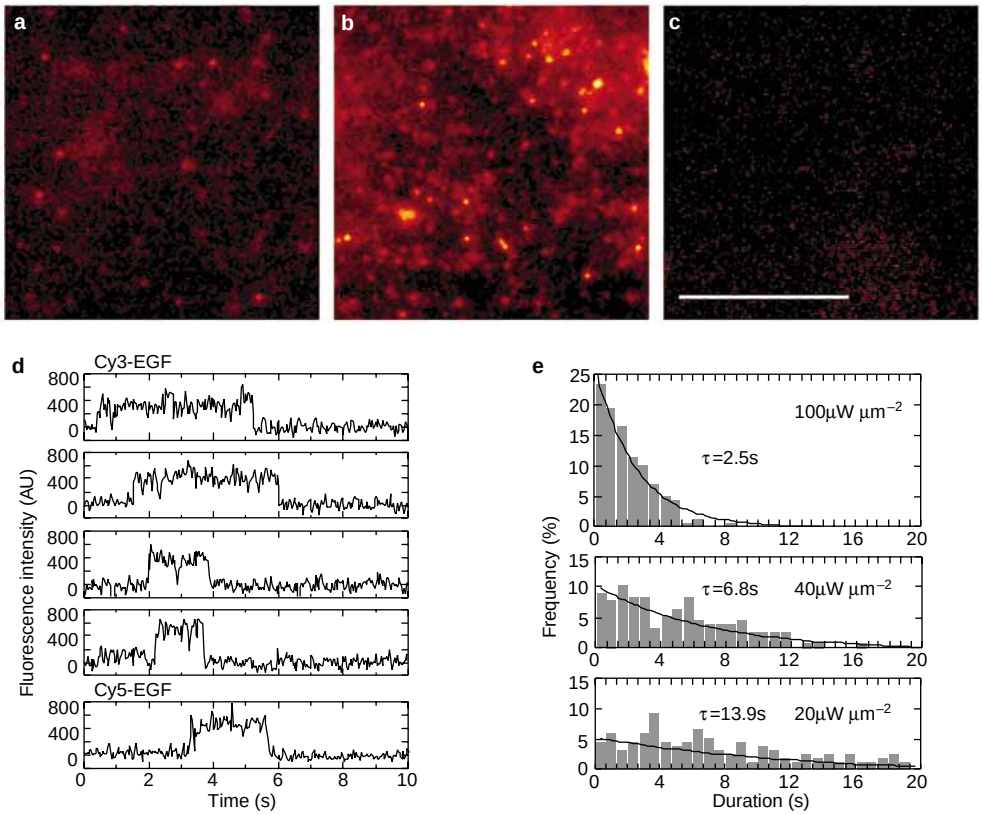

Figure 2 **Visualization of Cy3–EGF on the plasma membrane of living A431 cells. a**, **b**, Cy3–EGF at a final concentration of 0.2 ng ml^{-1} was added to the culture medium of living A431 cells under a TIR fluorescence microscope. Images were acquired immediately (**a**) and 1 min (**b**) after the addition of Cy3–EGF. **c**, A mixture of Cy3–EGF (0.2 ng ml^{-1}) and EGF (200 ng ml^{-1}) was added to the culture medium of A431 cells. This image was acquired 1 min after the addition of Cy3–EGF and EGF. Scale bar represents 10 μm. **d**, The change in fluorescence intensity of individual Cy3 (or Cy5)–EGF spots on living cells was measured frame by frame (30 frames every second) and plotted against time. An HeNe laser (632.8 nm) was used for observation of Cy5–EGF. AU, arbitrary unit. **e**, Histograms of the time difference between the appearance and disappearance of Cy3–EGF spots under lasers of variable excitation powers. The lines represent the fitting of the results to a single exponential function. τ indicates the time constant of the fit function. Multiple correlation coefficients (*R*) of the fitting are 0.991 (100 μW μm^{-2}), 0.916 (40 μW μm^{-2}) and 0.741 (20 μW μm^{-2}).

cence of cells before addition of Cy3–EGF was low, except at large vesicles in the perinuclear region. Soon after the addition of Cy3–EGF, fluorescent spots appeared on the cell surface; the density of these spots increased with time (Fig. 2a, b). Cy3–EGF was not detectable as fluorescent spots in the culture medium because of brownian movement in solution. In addition, the background fluorescence caused by Cy3–EGF in the medium was low because of the low excitation depth of TIR microscopy. Binding of Cy3–EGF to the cell surface was completely inhibited by addition of excess unlabelled EGF at the same time that Cy3–EGF was added (Fig. 2c), indicating specific binding of Cy3–EGF to the cell-surface EGFR. Cy3–EGF did not bind to CHO-K1 cells, which lack EGFR[6] (data not shown).

By carefully adjusting the incident angle of the excitation laser beam, we were able to visualize Cy3–EGF on both apical and basolateral plasma membranes by TIR microscopy (Fig. 1b, c). A slight difference in the refractive indices of the cytoplasm and the culture medium resulted in imaging of the apical surface of the cell membrane. Here we studied mainly the apical surface (see Supplementary Information).

We followed the change in fluorescence intensity of each Cy3–EGF spot in living A431 cells (Fig. 2d). In many cases, a spot appeared suddenly on the cell surface, emitted almost constant fluorescence, then disappeared suddenly. Histograms of the time difference between the appearance and the disappearance of each spot were well fit with a single exponential function. The inverse of the lifetime is proportional to the excitation laser power (Fig. 2e). This relationship between the lifetime and excitation power indicates that the duration of fluorescence was determined by the rate of photobleaching of Cy3–EGF. Thus it is likely that the sudden disappearance of the Cy3–EGF spots was caused by photobleaching, not by dissociation from EGFR or by endocytosis into the cytoplasm. Single-step photobleaching is strong evidence that the fluorescent spots represented single Cy3–EGF molecules on the cell surface[1].

We conjugated a monoclonal anti-EGFR antibody (EGFR1) with Cy3 (generating Cy3–EGFR1), and allowed this to bind to A431 cells in the same way as Cy3–EGF. The concentration of Cy3–EGFR1 was low (0.1 μg ml^{-1}) so as not to induce aggregation of EGFR. As EGFR1 can be labelled with multiple Cy3 molecules, the intensity distribution of Cy3–EGFR1 spots on the cell surface was fitted to a sum of two or three Gaussian distribution functions (Fig. 3b, c). The results of this fitting are consistent with Poisson distributions of the number of Cy3 molecules to EGFR1 molecules, indicating that the first, the second and the third components represent EGFR1 conjugated with one, two or three Cy3 molecules, respectively.

As, in the intensity distribution of Cy3–EGF (Fig. 3a), the mean of the first component was the same as those for Cy3–EGFR1, we conclude that this component contains single Cy3–EGF molecules. Binding of EGF to EGFR induces dimerization of EGFR[4], which is indispensable for EGF signalling. The second component, which emits a signal twice as intense as the first component, may represent

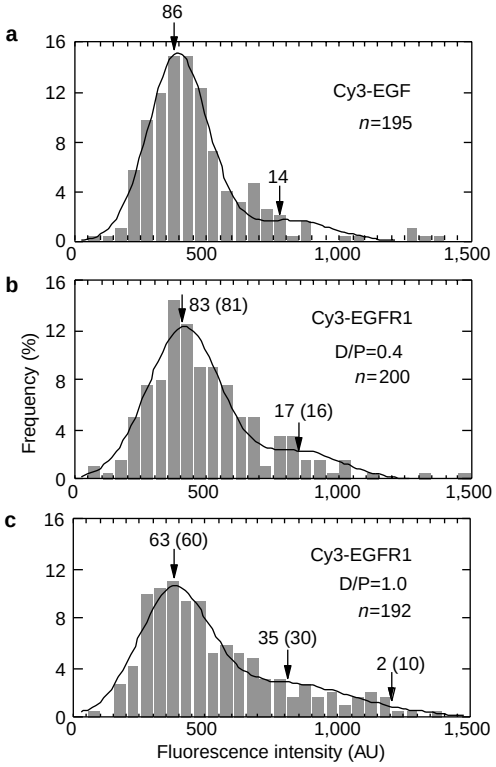

Figure 3 **Distribution of the fluorescence intensity of Cy3–EGF and Cy3–EGFR1 1 on the surface of living cells.** As well as Cy3–EGF (**a**), two preparations of Cy3-labelled anti-EGFR antibody (Cy3–EGFR1; final concentration of 0.1 μg ml^{-1}; **b**, **c**) with different average dye:protein ratios (D/P) were applied to A431 cells. Histograms of the fluorescence intensity were fit to a sum of two (**a**, **b**) or three (**c**) Gaussian distributions (lines). The peak, mean and standard deviation of Gaussian functions were fit. No parameter was forced on another. The positions of the mean (arrows) and percentage of the fraction (numbers not in parentheses) of each Gaussian component are indicated. Numbers in parentheses are the percentage of the fractions expected from Poisson distributions with average of 0.4 (**b**) and 1.0 (**c**). Multiple correlation coefficients (*R*) of the fitting are 0.967 (**b**) and 0.977 (**c**).

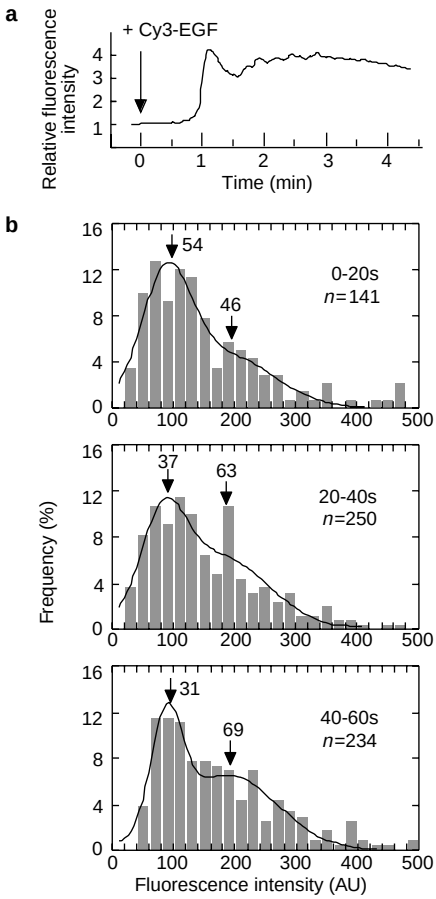

Figure 4 **Intracellular Ca^{2+} response induced by Cy3–EGF and the change in intensity distribution of Cy3–EGF spots. a**, Cells were loaded with the fluorescent Ca^{2+} indicator Fluo-3 (Dojindo, Kumamoto, Japan). At time 0, 1 ng ml^{-1} Cy3–EGF was added to the culture medium at 25 °C. The increase in the fluorescence intensity of Fluo-3 over time indicates an increase in the concentration of intracellular Ca^{2+}. **b**, Fluorescence-intensity distributions of Cy3–EGF spots were studied at various times after the addition of Cy3–EGF. The experimental conditions were the same as those for **a**. The fluorescence intensity of the spots was measured in 11–15 single-frame snapshots of different cells during each period. Results were fitted to a sum of two Gaussian distributions (line), and the percentages of fractions of each component are indicated (numbers). The peak, mean and standard deviation of Gaussian functions were fit. No parameter was forced on another. Multiple correlation coefficients (*R*) of the fitting are 0.945 (0–20 s), 0.933 (20–40 s) and 0.954 (40–60 s). The distributions at 20–40 s and 40–60 s are statistically similar to the distribution at 0–20 s, with a significance (*P*) of 0.38 and 0.0065, respectively (Mann–Whitney *U*-test). Densities of the Cy3–EGF spots on the cell surface were 0.18, 0.38 and 0.42 per μm^2 at 0–20, 20–40 and 40–60 s, respectively.

two Cy3–EGF molecules bound to a dimer of EGFR or two EGFR monomers closer than the spatial resolution of the microscope. The latter proposal is less probable because of the low density of the fluorescent spots.

From the results shown in Figs 2, 3, we conclude that we had visualized single Cy3–EGF molecules on the surface of living cells. We visualized single molecules of EGF labelled with other fluorescent dyes, Cy5 (Fig. 2d) and tetramethylrhodamine (data not shown), by the same technique.

Single-molecule tracking of EGFR dimerization. The intracellular Ca^{2+} response induced by EGF requires dimerization of the receptor[7]. Thus, dimerization should take place before the increase in the intracellular Ca^{2+} concentration that we observed 1 min after the addition of Cy3–EGF (Fig. 4a). We studied the formation of the EGF–EGFR dimeric complexes by checking the intensity distribution of the fluorescent spots at various times after the addition of Cy3–EGF. The amount of the component containing two Cy3–EGF molecules increased 40–60 s after the addition of Cy3–EGF (Fig. 4b), as the density of cell-surface Cy3–EGF spots increased (Fig. 2a, b). This increase in levels of the fraction containing EGFR dimer before the increase in Ca^{2+} amounts was consistent with the theory that signal transduction from the EGFR occurs through EGFR dimerization.

Single-molecule visualization enables single-molecule tracking in living cells[8,9]. Using this technique, we traced the formation of fluorescent spots containing two Cy3–EGF molecules. In a few cases (3 out of 26), two spots diffusing laterally along the plasma membrane collided and then moved together (Fig. 5a, upper panel). However, in most cases (23 out of 26), the fluorescence intensity of a spot increased suddenly by a factor of about two, then decreased in two steps (Fig. 5a, lower panel, Fig. 5b). This result points to a dimerization between EGFR molecules that exists just before the binding of a second EGF molecule. It is probable that the preformed dimer, which could not be detected using previous methods[5,10–12], is formed before the second EGF molecule binds.

Usually, lateral mobility of Cy3–EGF spots on the cell surface was small; large-scale movement is not necessary for EGFR signalling. One reason for the restriction of lateral mobility of EGFR

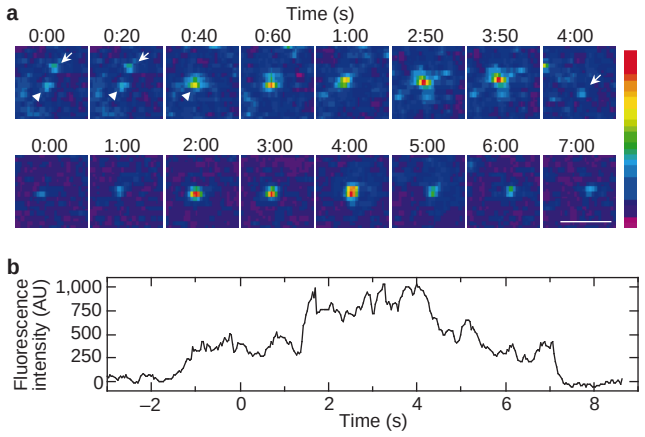

Figure 5 **Dimerization of EGF–EGFR complexes. a**, Under the same conditions as those used for Fig. 3a, the formation of Cy3–EGF spots with a signal intensity twice that of monomer spots was traced. In the upper panel, two spots (arrow and arrowhead) collided at time 0:40 s and then moved together. The fluorescence intensity increased after the collision. At 4:00 s, the intensity of the spot decreased to about half that at 3:50 s (arrow), probably because of photobleaching of one Cy3–EGF molecule. In the lower panel, a fluorescence spot with the intensity of a single molecule was observed until 1:00 s; intensity of the spot increased suddenly between 1:00 s and 2:00 s, then decreased between 4:00 s and 5:00 s. Scale bar represents 5 μm. **b**, Time trace of the fluorescence intensity of the spot shown in the lower panel of **a**. A two-step build-up and bleaching of intensity can be seen. The time trace is noisy because of slow, lateral diffusive movement of the spot.

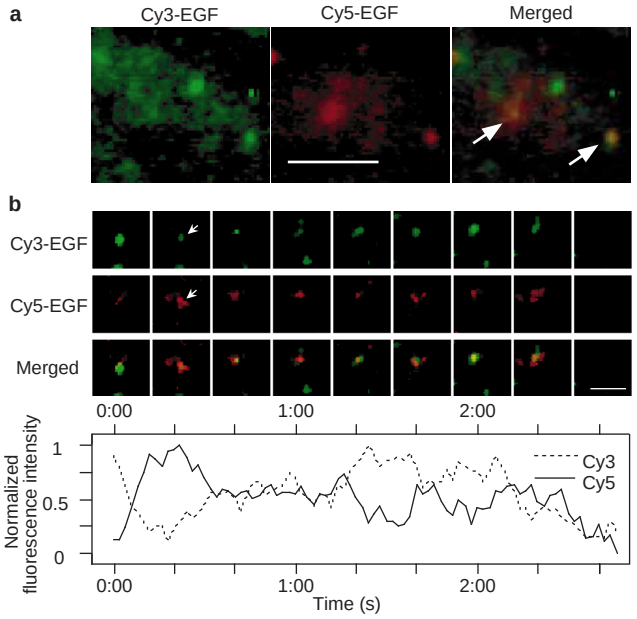

Figure 6 **Single-molecule FRET between Cy3–EGF and Cy5–EGF. a**, A mixture of Cy3–EGF (0.2 ng ml^{-1}) and Cy5–EGF (0.8 ng ml^{-1}) was added to the culture medium of A431 cells. The specimen was excited with a green (532 nm) laser beam and fluorescence images of the same field in the Cy3 channel (565–595 nm) and Cy5 channel (650–690 nm) were acquired simultaneously by using dual-view optics. Fluorescent spots shown in the Cy5 channel appeared as a result of FRET from Cy3–EGF to Cy5–EGF (arrows). **b**, Top three rows, the change in fluorescence intensity over time of a single spot (arrow) was measured in both Cy3 and Cy5 channels. The position of the spot moved slowly, probably because of slow brownian movement of cytoskeleton-bound membrane proteins[25]. To avoid photobleaching, the excitation laser power was reduced to 10 μW μm^{-2} and images were acquired using a four-frame rolling average. Bottom, the fluorescence intensities in Cy3 and Cy5 channels were plotted against time after normalization with respect to the peak intensity of each channel. Anti-correlation between Cy3 and Cy5 fluorescence intensities indicates FRET from Cy3 to Cy5.

is binding to the cytoskeleton[13,14].

Single-molecule fluorescence-resonance energy-transfer analysis. We measured molecular-level interactions of EGF in an EGFR dimer by single-molecule fluorescence-resonance energy transfer (FRET)[2,15]. We added a mixture of Cy3–EGF and Cy5–EGF to the cells, excited Cy3–EGF with a 532-nm laser, and acquired fluorescence images at 580 nm (for Cy3) and 670 nm (for Cy5) simultaneously by using dual-view optics[16] (Fig. 6a). Anti-correlation of the fluorescence-intensity changes of the same spot in the Cy3 channel and the Cy5 channel indicated FRET from Cy3–EGF to Cy5–EGF, that is, single-molecular detection of interaction between EGF molecules in a dimer (Fig. 6b). Fluctuation of the FRET efficiency may be caused by conformational fluctuation of the dimer. The low mobility of the dimer shown in Fig. 6b was compatible with the fact that micrometre-scale lateral mobility is not necessary for dimerization and signalling of the EGFR.

The probability of detecting FRET (10/201 = 5%) was lower than that expected from the histograms shown in Fig. 4. The distance between Cy3 and Cy 5 in a dimeric EGF–EGFR complex may be longer than the Förster distance between a Cy3–Cy5 pair (5.8 nm)[15] (see Supplementary Information).

Detection of autophosphorylation of EGFR. Dimerization of the EGFR induces autophosphorylation on its cytoplasmic tyrosine residues[5]. A monoclonal antibody, mAb74, recognizes the conformational change of the cytoplasmic domain of EGFR that is induced by autophosphorylation[17]. We perforated A431 cells with streptolysin O[18] to introduce Cy3-labelled mAb74 (Cy3–mAb74) into the cytoplasm. After stimulating the cells with Cy5–EGF, we visualized the binding of Cy3–mAb74 to the plasma membrane. Fluorescent spots of Cy3–mAb74 co-localized with the spots of Cy5–EGF that had a signal about twice as intense of that of other Cy5–EGF spots, indicating autophosphorylation of EGFR after dimerization (Fig. 7). This result is consistent with a widely accepted hypothesis for the mechanism of EGFR activation, that is, that formation of a dimeric EGF–EGFR complex induces autophosphorylation of EGFR.

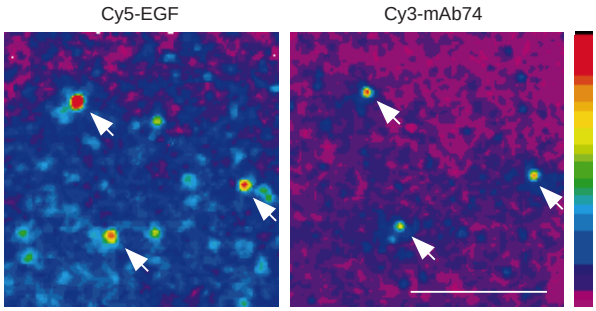

Figure 7 **Phosphorylation of EGF–EGFR complexes.** A431 cells were perforated using streptolysin O and stimulated with 10 ng ml^{-1} Cy5–EGF for 1 min. Phosphorylation of the EGFR was detected with Cy3–mAb74 (mAb74 is an antibody that recognizes activated (phosphorylated) EGFR). Images were acquired 15 min after the addition of Cy3–mAb74 using dual-view optics. Cy3–mAb74 bound at the positions indicated by the bright Cy5–EGF spots (arrows). Scale bar represents 10 μm.

Discussion

Here, using single-molecule imaging techniques, we have been able to detect the location, movement, interaction and biochemical reaction of single EGFR molecules. Our results indicate the presence of a preformed EGFR dimer and conformational fluctuation of this dimer.

Despite the fact that dimerization of the EGFR is known to be essential for signal transduction, the process of dimerization has not been fully understood. Our results indicate that EGF–$(EGFR)_2$ complexes are formed before the second EGF molecule binds. It has been reported that the binding of EGF to an EGFR dimer is more than ten times stronger than EGF binding to an EGFR monomer[19–21]. This is probably the reason why the second EGF molecule bound effectively bound to EGF–$(EGFR)_2$ in our experiments, even though there might be many unoccupied EGFR monomers on the cell surface. It has been suggested that hetrodimerization between EGFR-related receptors (ErbB2 and ErbB3) is induced by bivalency of a ligand, the differentiation factor Neu[22]. Dimerization of the EGFR may similarly be induced by bivalent binding of EGF. A twisted model has been proposed for dimerization of the EGFR[12]. In this model, binding of EGF activates the EGFR by inducing a twisting of a preformed EGFR dimer. Our results are consistent with this model. Another possible interpretation of our results is that dimerization occurs between EGFR molecules corralled into the dense membrane cytoskeletal network[23–25].

On the cell surface, EGFR molecules with high ($K_d < 1$ nM) and low ($K_d > 10$ nM) affinity for EGF are present. At the concentration of Cy3–EGF used in our experiments (0.2 nM), high-affinity EGFR, which is responsible for signal transduction[13], was mainly visualized. The activation of low-affinity receptors may occur in different ways. The conformational fluctuation of EGFR dimers is also suggested by the results of our single-molecule experiments. It is possible that the EGFR dimer can exist in several different conformations. Future work will address the relationship between the conformation and activity of EGFR dimers.

Finally, monitoring the behaviour and reaction of signal-transduction molecules using single-molecule techniques will be indispensable in fully understanding the mechanism of intracellular signalling. □

Methods

Cell culture.

A human carcinoma cell line, A431, was used 2 days after transfer of cells to a subculture. Before the experiments, culture medium was exchanged to that without serum and phenol red overnight.

Fluorescence labelling of proteins.

Recombinant mouse EGF (Higeta, Tokyo, Japan) was reacted with an *N*-hydroxysuccinidimyl ester of Cy3 or Cy5 (Amersham) according to the manufacturer's instructions. After a gel filtration using Sephadex G-15 (Pharmacia) to remove unreacted dye, Cy3 (or Cy5)-tagged EGF was further purified by reversed-phase column chromatograph[26]. A fraction with a dye:protein ratio of 0.9–1.1 was used. Mouse monoclonal anti-EGFR antibodies (EGFR1 (Genosys) and mAb74 (Transduction Laboratories)) were conjugated with Cy3 by the method used to label EGF. These antibodies can be labelled with multiple Cy3 molecules.

TIR microscopy.

We used an objective-type TIR fluorescence microscope[3] based on an inverted microscope (IX-70, Olympus) equipped with an oil-immersion objective (PlanApo ×60, NA 1.4, Olympus). Specimens were illuminated with a SHG-Nd/YAG laser (model 142-0532-100, Lightwave, Mountain View, USA) with an excitation power density of 10–100 $\mu W \mu m^{-2}$. Images of the specimens were intensified by a microchannel plate (VS4-1845; Video Scope, Sterling, USA) and acquired by a chilled charge-coupled-device (CCD) camera (C5985; Hamamatsu, Hamamatsu, Japan) at video rate.

Detection of EGFR phosphorylation.

Cells were perforated with streptolysin O, and incubated with 20 U ml^{-1} calf thymus alkaline phosphatase (Roche Molecular Biochemicals) in transport buffer (20 mM HEPES-KOH (pH 7.3), 110 mM CH_3COOK, 5 mM CH_3COONa, 2 mM $(CH_3COO)_2Mg$, 1 mM EGTA, 1 mM dithiothreitol) for 30 min at 37 °C. After washing the cells twice with transport buffer, we stimulated the EGFR with 10 ng ml^{-1} Cy5–EGF in the presence of 1 mM ATP for 1 min at room temperature. The remaining Cy5–EGF in the medium was washed out, and cells were incubated with Cy3–mAb74 in the presence of 1 mM ATP in transport buffer containing 1% bovine serum albumin.Cy3 and Cy5 were excited simultaneously by two lasers (532 and 632.8 nm). Fluorescence signals from Cy3 and Cy5 were separated by two dichroic mirrors (600 nm) and band-pass filters (565–595 nm for Cy3, and 650–690 nm for Cy5) in the dual-view optics. No crosstalk between the Cy3 and Cy5 channels was observed under this optical set-up.

RECEIVED 16 SEPTEMBER 1999; REVISED 29 DECEMBER 1999; ACCEPTED 21 JANUARY 2000; PUBLISHED 10 FEBRUARY 2000.

1. Funatsu, T., Harada, Y., Tokunaga, M., Saito, K. & Yanagida, T. Imaging of single fluorescent molecules and individual ATP turnovers by single myosin molecules in aqueous solution. *Nature* **374,** 555–559 (1995).
2. Weiss, S. Fluorescence spectroscopy of single biomolecules. *Science* **283,** 1676–1683 (1999).
3. Tokunaga, M., Kitamura, K., Saito, K., Hikikoshi-Iwane, A. & Yanagida, T. Single molecule imaging of fluorophores and enzymatic reactions achieved by objective-type total internal reflection fluorescence microscopy. *Biochem. Biophys. Res. Commun.* **235,** 47–53 (1997).
4. Yarden, Y. & Schlessinger, J. Epidermal growth factor induces rapid, reversible aggregation of the purified epidermal growth factor receptor. *Biochemistry* **26,** 1443–1451 (1987).
5. Yarden, Y. & Schlessinger, J. Self-phosphorylation of epidermal growth factor receptor: evidence for a model of intermolecular allosteric activation. *Biochemistry* **26,** 1434–1442 (1987).
6. Chung, C., Sciaky, N. & Gross, D. J. Heterogeneity of epidermal growth factor binding kinetics on individual cells. *Biophys. J.* **73,** 1089–1102 (1997).
7. Carraway, K. L. III & Cerione, R. A. Comparison of epidermal growth factor (EGF) receptor-receptor interactions in intact A431 cells and isolated plasma membrane. *J. Biol. Chem.* **266,** 8899–8906 (1991).
8. Schütz, G. J., Schindler, H. & Schmidt, T. H. Single-molecule microscopy on model membranes reveals anomalous diffusion. *Biophys. J.* **73,** 1073–1080 (1997).
9. Ide, T. & Yanagida, T. An artificial lipid bilayer formed on an agarose-coated glass for simultaneous electrical and optical measurement of single ion-channels. *Biochem. Biophys. Res. Commun.* **265,** 595–599 (1999).
10. Azevedo, J. R. & Johnson, D. A. Temperature-dependent lateral and transverse distribution of the epidermal growth factor receptor in A431 plasma membranes. *J. Memb. Biol.* **118,** 215–224 (1990).
11. Zidovetzki, R., Yarden, Y., Schlessinger, J. & Jovin, T. M. Microaggregation of hormone-occupied epidermal growth factor receptors on plasma membrane preparations. *EMBO J.* **5,** 247–250 (1986).
12. Gadella, T. W. J. Jr & Jovin, T. M. Oligomerization of epidermal growth factor receptors on A 431 cells studied by time-resolved fluorescence imaging microscopy. A stereochemical model for tyrosine kinase receptor activation. *J. Cell Biol.* **129,** 1543–1558 (1995).
13. den Hartigh, J. C., van Bergen en Henegouwen, P. M., Verkleij, A. J. & Boonstra, J. The EGF receptor is an actin-binding protein. *J. Cell Biol.* **119,** 349–355 (1992).
14. Wiegant, F. A. C. *et al.* Epidermal growth factor receptors associated to cytoskeletal elements of epidermoid carcinoma (A431) cells. *J. Cell Biol.* **103,** 87–94 (1986).
15. Ishii, Y., Yoshida, T., Funatsu, T., Wazawa, T. & Yanagida, T. Fluorescence resonance energy transfer between single fluorophores attached to a coiled-coil protein in aqueous solution. *Chem. Phys.* **247,** 163–173 (1999).
16. Kinoshita, K., Itoh, H., Ishiwata, S., Nishizaka, T. & Hayakawa, T. Dual-view microscopy with a single camera: real-time imaging of molecular orientations and calcium. *J. Cell Biol.* **115,** 67–73 (1991).
17. Campos-González, R. & Glenney, J. R. Jr Immunodetection of the ligand-activated receptor for epidermal growth factor. *Growth Factors* **4,** 305–316 (1991).
18. Pimplikar, S. W., Ikonen, E. & Simons, K. Basolateral protein transport in streptolysin O-permeabilized MDCK cells. *J. Cell Biol.* **125,** 1025–1035 (1994).
19. Lemmon, M. A. *et al.* Two EGF molecules contribute additively to stabilization of the EGFR dimer. *EMBO J.* **16,** 281–294 (1997).
20. Hurwitz, D. R. *et al.* EGF induces increased ligand binding affinity and dimerization of soluble epidermal growth factor (EGF) receptor extracellular domain. *J. Biol. Chem.* **266,** 22035–22043 (1991).
21. Sorokin, A., Lemmon, A., Ullrich, A. & Schlessinger, J. Stabilization of an active dimeric form of the epidermal growth factor receptor by introduction of an inter-receptor disulfide bond. *J. Biol. Chem.* **269,** 9752–9759 (1994).
22. Tzahar, E. *et al.* Bivalence of EGF-like ligands drives the ErbB signaling network. *EMBO J.* **16,** 4938–4950 (1997).
23. Sako, Y. & Kusumi, A. Barriers for lateral diffusion of transferrin receptor in the plasma membrane as characterized by receptor dragging by laser tweezers: fence versus tether. *J. Cell Biol.* **129,** 1559–1574 (1995).
24. Kusumi, A. & Sako, Y. Cell surface organization by the membrane skeleton. *Curr. Opin. Cell Biol.* **8,** 566–574 (1996).
25. Sako, Y., Nagafuchi, A., Tsukita, S., Takeichi, M. & Kusumi, A. Cytoplasmic regulation of the movement of E-cadherin on the free cell surface as studied by optical tweezers and single particle tracking: corralling and tethering by the membrane skeleton. *J. Cell Biol.* **140,** 1227–1240 (1998).
26. Carraway, K. L. III, Koland, J. G. & Cerione, R. A. Visualization of epidermal growth factor (EGF) receptor aggregation in plasma membranes by fluorescence resonance energy transfer. Correlation of receptor activation with aggregation. *J. Biol. Chem.* **264,** 8699–8707 (1989).

ACKNOWLEDGEMENTS

We thank T. Wazawa at the Single-Molecular Processes Project for the computer program with which to measure fluorescence intensity; M. Murata for streptolysin O; and P. Conibear and F. Brozovich for critical reading of the manuscript.

Correspondence and requests for materials should be addressed to T.Y.

Supplementary information is available on *Nature Cell Biology*'s World-Wide Web site (http://cellbio.nature.com) or as paper copy from the London editorial office of *Nature Cell Biology*.